Alexandria Engineering Journal (2016) xxx, xxx–xxx

HOSTED BY

Alexandria University

Alexandria Engineering Journal

www.elsevier.com/locate/aej
www.sciencedirect.com

ORIGINAL ARTICLE

MHD squeezed flow of Carreau-Yasuda fluid over a sensor surface

T. Salahuddin *, **M.Y. Malik, Arif Hussain, S. Bilal, M. Awais, Imad Khan**

Department of Mathematics, Quaid-i-Azam University, Islamabad 44000, Pakistan

Received 26 June 2016; revised 16 August 2016; accepted 29 August 2016

KEYWORDS

MHD flow;
Carreau-Yasuda fluid;
Squeezed flow;
Sensor surface;
Runge-Kutta-Fehlberg method

Abstract An attempt has been made to examine the two dimensional free stream squeezed flow through a horizontal sensor surface of an electrically conducting Carreau-Yasuda fluid subject to transverse magnetic field. The governing nonlinear partial differential equations are modeled and then simplified with the aid of suitable similarity transformations. Well known numerical scheme Runge–Kutta–Fehlberg method is utilized to solve the system. Concrete graphical analysis is carried out to investigate the behavior of different pertinent parameters on velocity profile with inclusive discussion. Numerical influence of friction factor is also discussed.

1. Introduction

Due to immense industrial and engineering applications, it is supreme interest to examine the magneto-hydrodynamic flow. The main purpose of magneto-hydrodynamic principles is to disturb the flow field in a preferred direction by varying the structure of the boundary layer. Thus, in order to amend the flow kinematics, the idea to implement MHD appears to be more easy and consistent. In medicine and biology, MHD has been receiving emergent attention of physiologists, fluid dynamicists and medical practitioners, due to its significance in biomedical engineering as well as in the cure of various pathological circumstances. Further example that fits to the above class of problems is modern metallurgical and metal-working processes. Mukhopadhyay [1] studied the MHD flow of viscous fluid induced due to exponentially stretching sheet. She obtained the solution of velocity and temperature functions by shooting method. Moreover, she found that as the magnetic field increases the surface shear stress enhances. Jat et al. [2] discussed the heat transfer flow of viscous fluid over an exponentially stretching sheet under the influence of radiation, viscous dissipation and magnetic force. They found that heat transfer rate enriches as the magnetic field increases. Desale et al. [3] carried out an investigation to see the effect of boundary layer MHD flow over a nonlinear stretching sheet. They concluded that the influence of magnetic field in reduction of velocity profile is more prominent than nonlinear stretching parameter. Uddin et al. [4] explored the numerical solution of MHD nonlinear nanomaterial stretching or shrinking sheet along with convective heating and Navier slip conditions. They illustrated that by increasing magnetic field the concentration and temperature profiles enhance. Awais et al. [5] discussed the MHD peristaltic flow of Jeffery fluid in an asymmetric channel with convective boundary conditions. They calculated the solution by using long wavelength approximation. Hayat et al. [6] studied the MHD peristaltic flow of

* Corresponding author.
E-mail address: taimoor.salahuddin@math.qau.edu.pk (T. Salahuddin).

Peer review under responsibility of Faculty of Engineering, Alexandria University.

http://dx.doi.org/10.1016/j.aej.2016.08.029

nanofluid in a channel with slip, wall properties and Joule heating. They found that both the nanoparticles concentration and temperature are increasing functions of thermophoresis and Brownian motion parameters. Akbar et al. [7] investigated the numerical solution of MHD Eyring-Powell fluid over a stretching sheet and found that the increment in magnetic field and Eyring–Powell fluid parameters reduces the velocity profile. Mabood et al. [8] analyzed the effects of MHD and viscous dissipation over a non-linear stretching sheet. They concluded that local Nusselt and Sherwood numbers reduces by increasing magnetic field. Hakeem et al. [9] examined the numerical solution for the MHD flow of nanofluid towards a stretching sheet with thermal radiation and second order slip conditions. They initiated that the second order slip and magnetic field have imperative influence on both shrinking and stretching sheet. By increasing the magnetic field the lower branch solution of shrinking sheet disappears. Sheikh et al. [10] discussed the heat generation/absorption and thermophoresis effects on MHD flow over an oscillatory stretching sheet. They effectuated that motion of the fluid deaccelerates by increasing magnetic field. Malik et al. [11] deliberated the solution of MHD flow of Williamson fluid towards a stretching cylinder by using shooting method. They found that velocity profile reduces by increasing magnetic field and Williamson parameter. Ali et al. [12] deliberated the numerical and analytical solutions of radially non-linear stretched surface with slip effects. They compared analytic and numerical results of the problem. Mahanthesh et al. [13] discussed the MHD flow of nanofluid (Cu, Al_2O_3 and TiO_2) over a bidirectional non-linear stretching surface. They calculated the results for both non-linear and linear stretching sheet cases. Some other articles related to MHD flow are described in Refs. [14–23].

Researchers currently have concentrated considerably on sensor surface due to its importance in biological and chemical processes. Microcantilever is such an example which has the ability to detect various diseases or can be used to accurately sense many bio-warfare or hazardous agents. Khaled and Vafai [24] studied the role of sensor surface confined inside a squeezed channel. They inaugurated that by increasing the wall suction velocity and magnetic field the local Nusselt number enriches. Rashidi et al. [25] obtained approximate solutions for two-dimensional unsteady squeezing flow between two parallel plates. They concluded that homotopy analysis method provides good approximation for both strongly and weakly non-linear problems. Haq et al. [26] analyzed the hydromagnetic squeezed flow of nanofluid towards a sensor surface. They initiated that by raising the nanoparticle volume fraction the velocity profile reduces.

Most of the fluids used in industries are non-Newtonian [27–31]. In such fluids there is no linear relationship between stress and deformation rate. Examples of such fluids are pulps, molten polymers, animal blood, etc. Carreau-Yasuda fluid is such a model that predicts the shear thinning/thickening behavior. Hayat et al. [32] discussed the peristaltic flow of Carreau-Yasuda Fluid with slip effects in a curved channel. They found that increase in velocity slip parameter decreases the retrograde pumping and peristaltic regions. The peristaltic flow of Carreau–Yasuda fluid model in an asymmetric channel with Hall and Ohmic heating effects was studied by Hayat et al. [33]. They made a comparative study for viscous, Carreau, and Carreau-Yasuda fluids. Hayat et al. [34] discussed the mixed convective peristaltic transport of Carreau–Yasuda fluid with chemical reaction and thermal deposition. They studied the problem by assuming the large wavelength and small Reynolds number approximation.

The above literature review illustrates that no one has studied so far the unsteady MHD boundary layer flow of Carreau-Yasuda fluid over a horizontal sensor surface inward a squeezing horizontal channel. After employing the appropriate similarity transformations the required equation of motion is reduced into non-linear differential form. The numerical solution of the resulting equation is calculated through Runge-Kutta- Fehlberg method. Finally, the impact of dimensionless parameters on the flow streamlines and velocity profile along with the friction factor are discussed with the help of graphs and table.

2. Mathematical formulation

Consider unsteady two-dimensional Carreau-Yasuda fluid flow between two infinite parallel plates. The microcantilever sensor of length L is enclosed inside the channel and the upper surface of the channel is squeezed, but the lower surface is fixed. It is assumed that the height $h(t)$ is greater than the boundary layer thickness. The flow is driven by the external free stream velocity $U(x,t)$ and the magnetic field of strength B_m is applied normal to the channel as shown in Fig. 1.

The constitutive equation of Carreau-Yasuda fluid is

$$\boldsymbol{\tau} = \left[\mu_\infty + (\mu_0 - \mu_\infty)\left(1 + (\Gamma\dot{\gamma})^d\right)^{\frac{n-1}{d}}\right]\mathbf{A}_1, \tag{1}$$

in which, τ is the extra stress tensor, A_1 is the first Rivlin-Ericksen tensor, μ_0 is the zero shear rate viscosity, μ_∞ is the infinite shear rate, d, n and Γ are the Carreau-Yasuda fluid parameters and $\dot{\gamma}$ is defined as $\dot{\gamma} = \sqrt{2tr(D^2)}$, where $D = \frac{1}{2}[gradV + (gradV)^T]$. Here it is assumed that $\mu_\infty = 0$, then Eq. (1) takes the following form:

$$\boldsymbol{\tau} = \boldsymbol{\mu}_0[1 + (\Gamma\dot{\gamma})^d]^{\frac{n-1}{d}}\mathbf{A}_1, \tag{2}$$

According to the present situation following are the equations of continuity, momentum and free stream:

$$\frac{\partial u}{\partial x} + \frac{\partial v}{\partial y} = 0, \tag{3}$$

$$\frac{\partial u}{\partial t} + u\frac{\partial u}{\partial x} + v\frac{\partial u}{\partial y} = -\frac{1}{\rho}\frac{\partial p}{\partial x} + \nu\frac{\partial^2 u}{\partial y^2} + \frac{(n-1)\nu}{d}\Gamma^d(d+1) \times \left(\frac{\partial u}{\partial y}\right)^d\frac{\partial^2 u}{\partial y^2} - \frac{\sigma_m B_m^2}{\rho}u, \tag{4}$$

$$\frac{\partial U}{\partial t} + U\frac{\partial U}{\partial x} = -\frac{1}{\rho}\frac{\partial p}{\partial x} - \frac{\sigma_m B_m^2}{\rho}U, \tag{5}$$

where ν is the kinematic viscosity, p is the fluid pressure, u and v are the x-component and y-components of velocity respectively, ρ is the density, n is the power law index, σ_m is the electric charge density, d is the generalized parameter and Γ is the time constant.

Eq. (4) is valid within the boundary layer while Eq. (5) is the outer stream flow which is presumed to be inviscid. Therefore, this assumption is devalued when the sensor length is taken to be much closer to the channel's height. Momentum

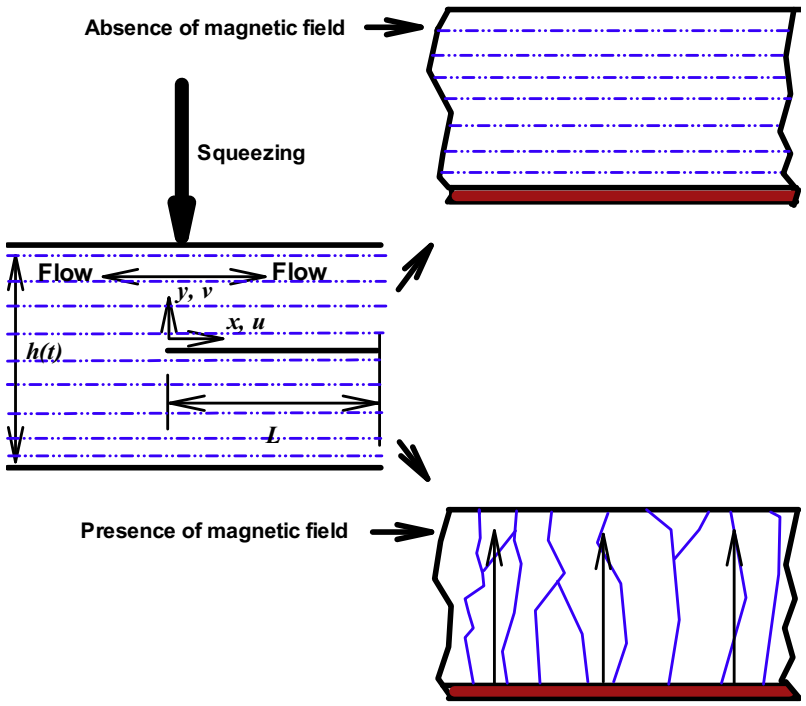

Figure 1 Flow configuration and coordinate system.

Eq. (4) takes the following form after eliminating the pressure gradient from Eq. (5):

$$\frac{\partial u}{\partial t}+u\frac{\partial u}{\partial x}+v\frac{\partial u}{\partial y}=\frac{\partial U}{\partial t}+U\frac{\partial U}{\partial x}+v\frac{\partial^2 u}{\partial y^2}+\frac{(n-1)v}{d}\Gamma^d(d+1)\times\left(\frac{\partial u}{\partial y}\right)^d\frac{\partial^2 u}{\partial y^2}+\frac{\sigma_m B_m^2}{\rho}(U-u), \tag{6}$$

the hydrodynamic boundary conditions for the problem can be written as follows:

$$u(x,0,t)=0,\quad v(x,0,t)=v_0(t),\quad u(x,\infty,t)=U(x,t). \tag{7}$$

Eq. (6) can be transformed to ordinary differential form when the following conditions and variables are executed:

$$U=ax,\ \eta=y\left(\frac{a}{v}\right)^{1/2},\ a=\frac{1}{s+bt},\quad v_0(t)=v_i(a)^{1/2},\ f(\eta)=\frac{\Psi}{x(av)^{1/2}}. \tag{8}$$

where a is the strength of squeeze flow but b is arbitrary constant. Eq. (8) displays that the motion of the channel's height is according to the following relation: $h(t)=h_0/(s+bt)^{1/b}$ and $h(t)=h_0e^{-st}$ for $b=0$ where h_0 is a constant. The surface permeable velocity enhances as the time reduces (when $b>0$), since squeezing velocity rises as time declines.

Now, substituting the transformations (8) into Eq. (6) to get similar equation of the form

$$f'''+f''\left(f+\frac{b\eta}{2}\right)-(f')^2+1+b(f'-1)+\frac{(n-1)(d+1)}{d}We^d(f'')^d f'''+M^2(1-f')=0, \tag{9}$$

for $d=2$ the problem reduces to Carreau fluid model but in this problem the value of Yasuda parameter d is taken to be 1. So Eq. (9) reduces to

$$f'''+f''\left(f+\frac{b\eta}{2}\right)-(f')^2+1+b(f'-1)+2(n-1)Wef''f'''+M^2(1-f')=0, \tag{10}$$

the transformed boundary conditions take the following form:

$$f(0)=0,\quad f'(0)=-f_0,\quad f'(\infty)=1, \tag{11}$$

where $M^2=\frac{\sigma_m B_m^2}{\rho a}$ is the Hartmann number, f_0 is the permeable velocity parameter and $We^d=\left(ax\sqrt{\frac{a}{v}}\Gamma\right)^d$ is the Weissenberg number.

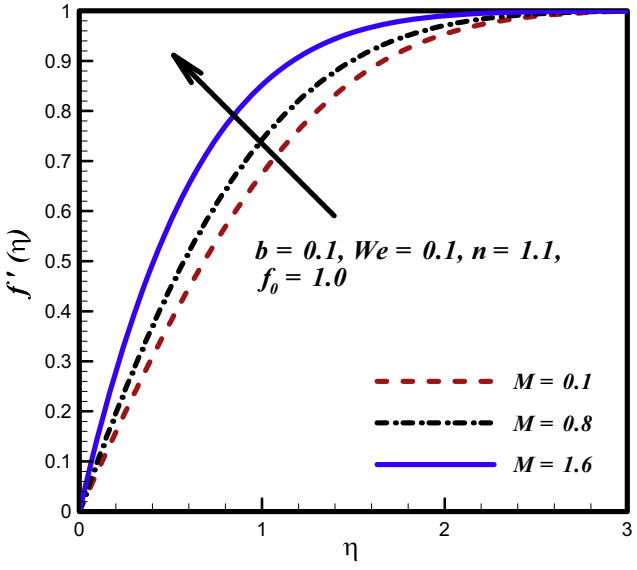

Figure 2 The influence of M on $f'(\eta)$.

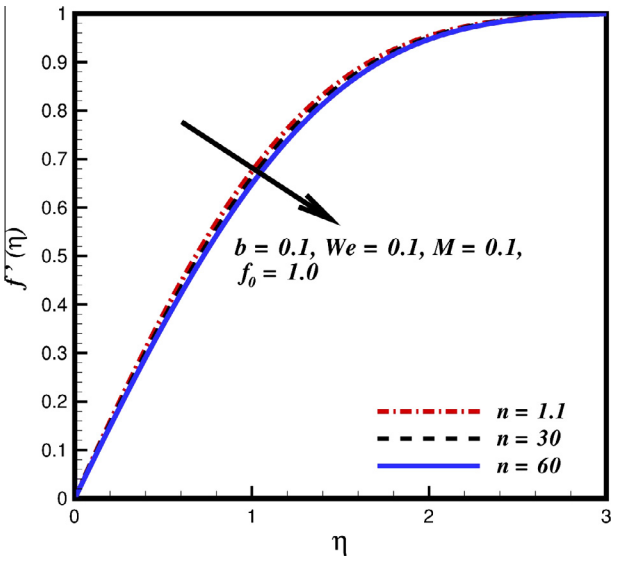

Figure 3 The influence of n on $f'(\eta)$.

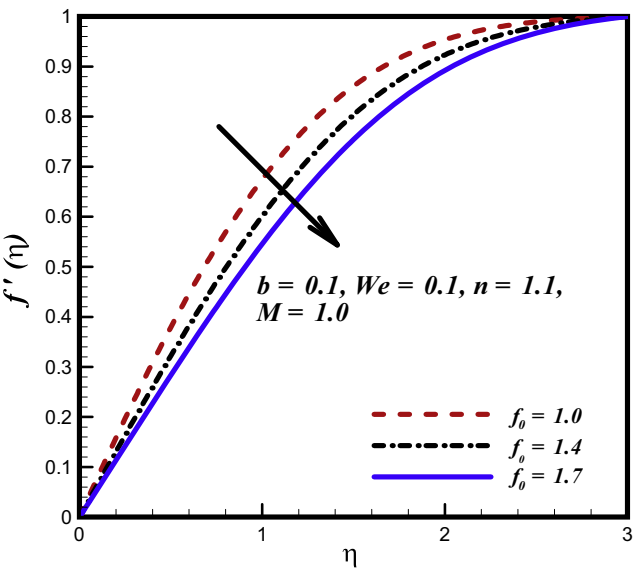

Figure 5 The influence of f_0 on $f'(\eta)$.

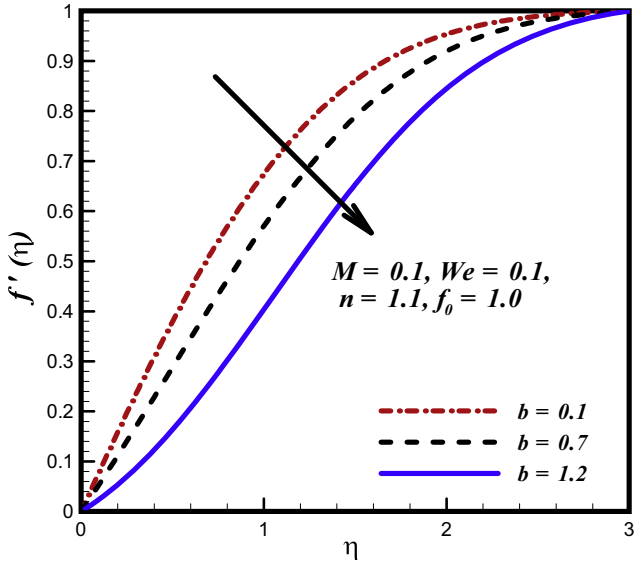

Figure 4 The influence of b on $f'(\eta)$.

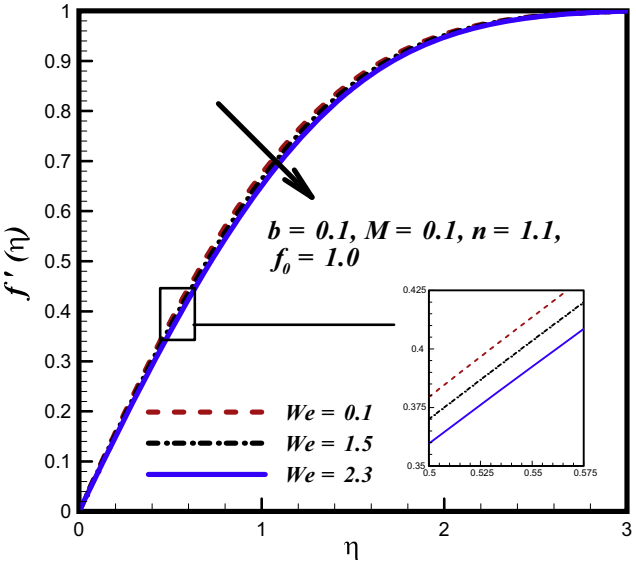

Figure 6 The influence of We on $f'(\eta)$.

In practical applications, the quantity of physical interest is to be determined. i.e. surface shear stress. This can be attained in terms of skin friction coefficient, from the subsequent relation,

$$C_f = \frac{2\tau_w}{\mu a Re^{1/2}} = f''(0) + (n-1)Wef''^2(0), \tag{12}$$

where μ is the dynamic viscosity, τ_w is the wall stress and $Re$is the Reynolds number.

3. Numerical method

The nonlinear momentum Eq. (10) subject to the boundary conditions (11) has been integrated numerically by using Runge-Kutta-Fehlberg method with shooting technique. For this purpose, the ordinary differential Eq. (10) is amended into following form:

$$f'''(1+2(n-1)Wef'') = -f''\left(f+\frac{b\eta}{2}\right) + (f')^2 - 1 - b(f'-1) - M^2(1-f'), \tag{13}$$

Transform the governing non-linear ordinary differential Eq. (13) to a system of first order differential equations as follows:

$$\begin{aligned} f &= m_1, \\ f' &= m_1' = m_2, \\ f'' &= m_2' = m_3, \end{aligned} \tag{14}$$

hence Eq. (13) becomes

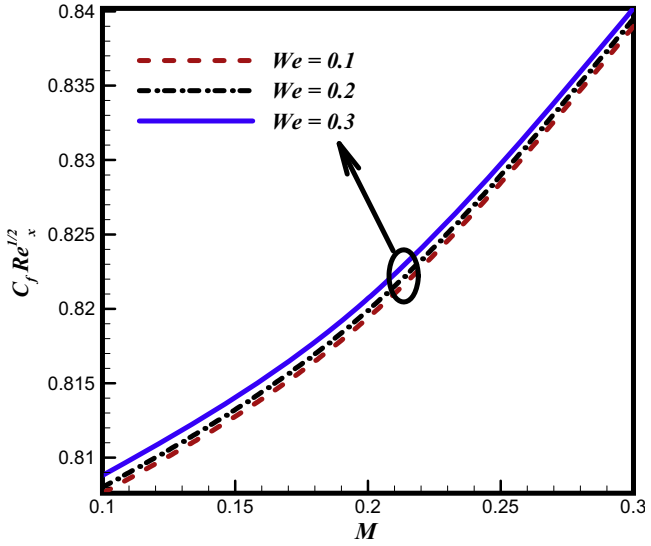

Figure 7 The influence of M and We on skin friction.

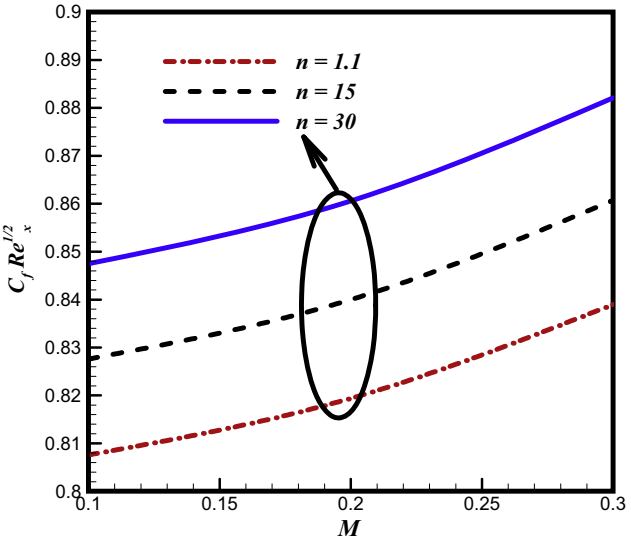

Figure 9 The influence of M and n on skin friction.

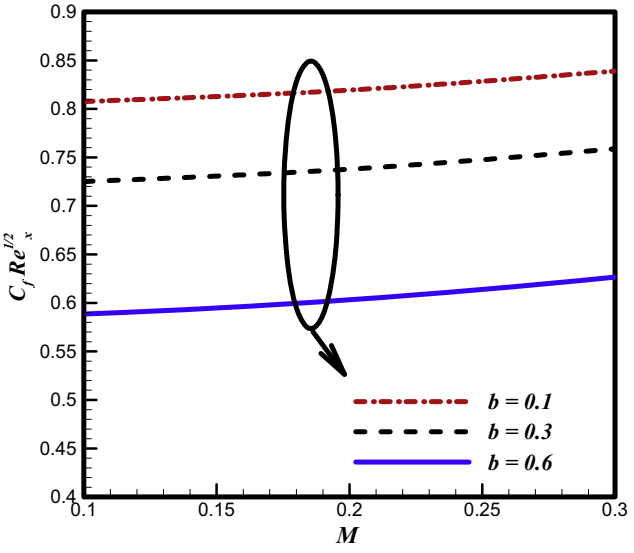

Figure 8 The influence of M and b on skin friction.

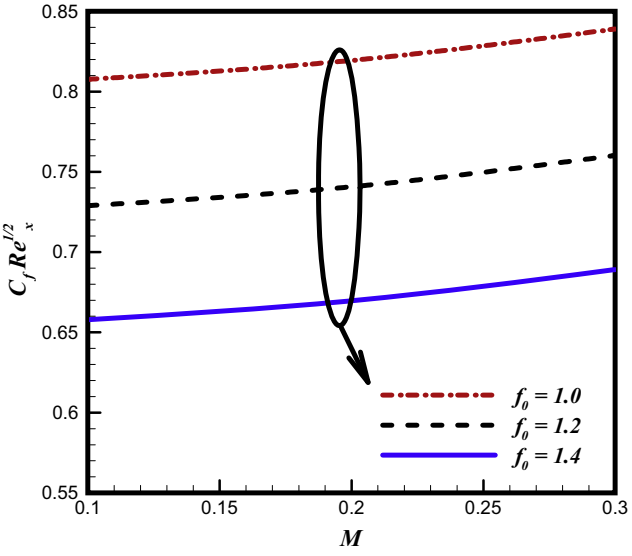

Figure 10 The influence of M and f_0 on skin friction.

$$m_3' = \frac{-m_3 m_1 - 0.5 b\eta m_3 + m_2^2 - b m_2 + b - M^2 + M^2 m_2}{1 + 2(n-1)We m_3}, \quad (15)$$

and the initial conditions are:

$$m_1(0) = 0, \quad m_2(0) = -f_0, \quad m_3(0) = u_1. \quad (16)$$

Here two initial conditions are requisite but one initial condition on m_3 is assumed. However, the value of m_3 is known at infinity. Thus, this end condition is utilized to produce one unknown initial condition at $\eta = 0$. The resulting initial value problem is solved by using the fifth order Runge–Kutta method. The Newton–Raphson method is also executed to correct the guessed values of $m_3(0)$.

4. Results and discussion

This section disquiets with the physical interpretation of different embedded physical parameters on flow streamlines, velocity and skin friction coefficient. The representative velocity profile for unlike values of Hartmann number M is displayed in Fig. 2. It is worth noting that the flow boundary layer thickness increases with each increment in Hartmann number M. Because by increasing Hartmann number M, the resistance in the flow direction increases but as the upper surface is squeezing this cancels the effect of Hartmann number M, so velocity profile increases. Fig. 3 illustrates the influence of power law index n on velocity profile. It is noticed that the boundary layer thickness and the velocity profile reduce by increasing power law index n. Fig. 4 shows the effect of

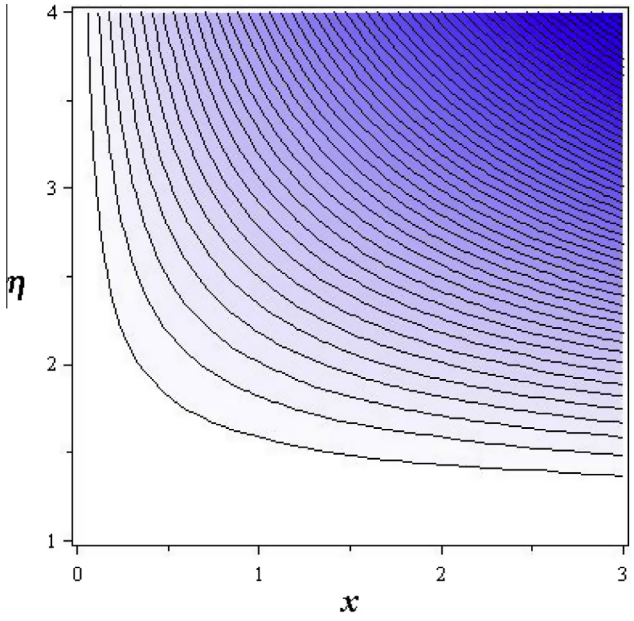

Figure 11 Stream lines for $M = 0.1$.

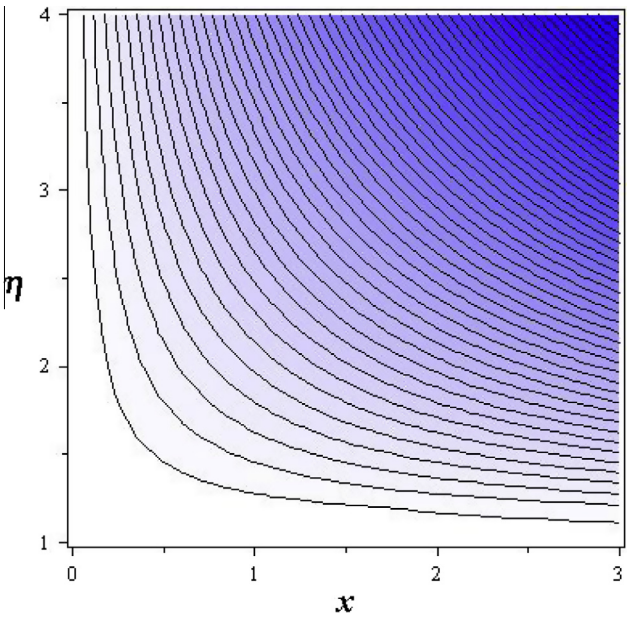

Figure 13 Stream lines for $M = 1.2$.

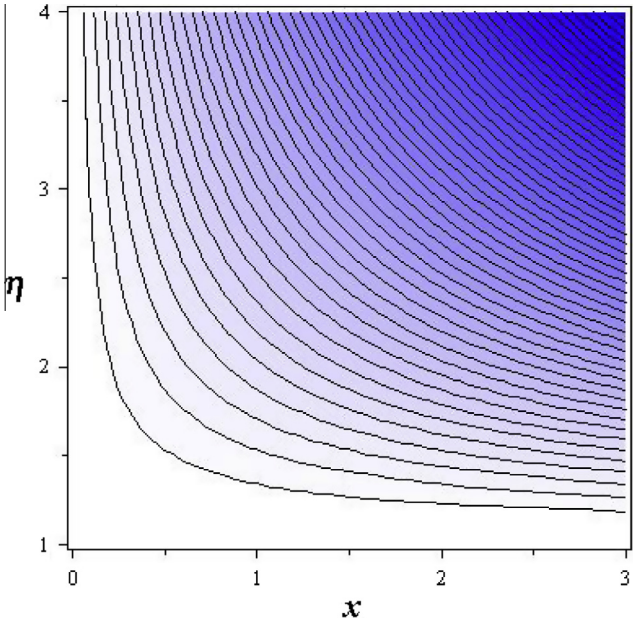

Figure 12 Stream lines for $M = 0.6$.

squeezed flow index b on velocity profile. This figure indicates that the velocity profile reduces for large values of squeezed flow index b. Because by increasing the squeezing phenomena the kinetic energy of the fluid particles enhances. But there is an inverse relation between strength of squeeze flow a and squeezed flow index b. So the velocity profile reduces. Fig. 5 depicts the influence of permeable velocity parameter f_0 on velocity profile. Because by increasing permeable velocity parameter f_0, suction takes place which affects the flow and hence velocity profile reduces. It is noticed that the velocity profile reduces for incremented values of permeable velocity parameter f_0. Fig. 6 captures the effect of Weissenberg number

Table 1 Numerical consequences of skin friction coefficient $f''(0) + (n-1)Wef''^2(0)$ for different values of M, b, We, n and f_0.

M	b	We	n	f_0	$f''(0) + (n-1)Wef''^2(0)$
0.1	0.1	0.1	1.1	1	0.8138
0.8	0.1	0.1	1.1	1	1.0466
1.6	0.1	0.1	1.1	1	1.6010
0.1	0.1	0.1	1.1	1	0.8138
0.1	0.7	0.1	1.1	1	0.5413
0.1	1.2	0.1	1.1	1	0.2269
0.1	0.1	1.5	1.1	1	0.8771
0.1	0.1	2.3	1.1	1	0.8933
0.1	0.1	0.1	1.1	1	0.8138
0.1	0.1	0.1	30	1	2.5388
0.1	0.1	0.1	60	1	4.1291
0.1	0.1	0.1	1.1	1	0.8138
0.1	0.1	0.1	1.1	1.4	0.6621
0.1	0.1	0.1	1.1	1.7	0.5686

We on velocity profile, the Weissenberg number We being the ratio of relaxation time to the specific process time. Bigger values of Weissenberg number We enhance the relaxation time of the fluid. Hence resistance in flow direction takes place causing velocity to drop.

The variation in skin friction coefficient C_f, given by Eq. (10), as a function of the Hartmann number M is shown in Figs. 7–10, for different values of Weissenberg number We, squeezed flow index b, power law index n and permeable velocity parameter f_0. Fig. 7 shows that for several values of Weissenberg number We, the magnitude of C_f increases with variation in Hartman number M. Fig. 8 depicts that the magnitude of C_f diminishes as the values of squeezed flow index b are increased. Fig. 9 portrays that each curve increases for different values of power law index n. Fig. 10 manifests that the magnitude of C_f reduces when permeable velocity parameter f_0 is incremented. Streamlines for several values of Hartmann

Please cite this article in press as: T. Salahuddin et al., MHD squeezed flow of Carreau-Yasuda fluid over a sensor surface, Alexandria Eng. J. (2016), http://dx.doi.org/10.1016/j.aej.2016.08.029

number M are shown in Figs. 11–13. It is analyzed that due to increase in Hartmann number M the streamlines are stretched towards x-axis. Finally, the disparity of skin friction coefficient C_f for dissimilar values of M, b, We, n and f_0 is shown in Table 1.

5. Conclusion

An investigation has been executed to examine the squeezed flow of Carreau-Yasuda fluid over a sensor surface in the presence of magnetic field . The effects are explored through graphs and table in order to demonstrate the parametric sensitivity of the flow. The outcomes pertaining to the present analysis are cataloged below:

- The presence of Hartmann number M enhances the boundary layer thickness and velocity profile.
- The velocity profile reduces by increasing squeezed flow index b.
- The skin friction coefficient at the surface enhances with increasing values of power law index n and Hartmann number M.
- The effect of permeable velocity parameter f_0 on velocity profile and skin friction coefficient is opposite.
- The increasing values of Weissenberg number We reduce the boundary layer and velocity profile.

References

[1] S. Mukhopadhyay, Slip effects on MHD boundary layer flow over an exponentially stretching sheet with suction/blowing and thermal radiation, Ain Shams Eng. J. 4 (2013) 485–491.
[2] R.N. Jat, G. Chand, MHD flow and heat transfer over a exponentially stretching sheet with viscous dissipation and radiation effects, Appl. Math. Sci. 7 (2013) 167–180.
[3] S.V. Desale, V.H. Pradhan, A study on MHD boundary layer flow over a nonlinear stretching sheet using implicit finite difference method, Int. J. Res. Eng. Technol. 2 (2013) 287–291.
[4] M.J. Uddin, A. Beg, N. Amin, Hydromagnetic transport phenomena from a stretching or shrinking nonlinear nanomaterial sheet with Navier slip and convective heating: a model for bio-nano-materials processing, J. Magnetism Magnetic Mater. 368 (2014) 252–261.
[5] M. Awais, S. Farooq, H. Yasmin, T. Hayat, A. Alsaedi, Convective heat transfers analysis for MHD peristaltic flow in an asymmetric channel, Int. J. Biomath., doi:http://dx.doi.org/10.1142/S1793524514500235.
[6] T. Hayat, Z. Nisar, Ahmad, H. Yasmin, Simultaneous effects of slip and wall properties on MHD peristaltic motion of nanofluid with Joule heating, J. Magnetism Magnetic Mater. 395 (2015) 48–58.
[7] N.S. Akbar, A. Ebaid, Z.H. Khan, Numerical analysis of magnetic field effects on Eyring-Powell fluid flow towards a stretching sheet, J. Magnetism Magnetic Mater. 382 (2015) 355–358.
[8] F. Mabood, W.A. Khan, A.I.M. Ismail, MHD boundary layer flow and heat transfer of nanofluids over a nonlinear stretching sheet: a numerical study, J. Magnetism Magnetic Mater. 374 (2015) 569–576.
[9] A.K.A. Hakeem, N.V. Ganesh, B. Ganga, Magnetic field effect on second order slip flow of nanofluid over a stretching/shrinking sheet with thermal radiation effects, J. Magnetism Magnetic Mater. 381 (2015) 243–257.
[10] M. Sheikh, Z. Abbas, Effects of thermophoresis and heat generation/absorption on MHD flow due to an oscillatory stretching sheet with chemically reactive species, J. Magnetism Magnetic Mater. 396 (2015) 204–213.
[11] M.Y. Malik, T. Salahuddin, Numerical solution of MHD stagnation point flow of Williamson fluid model over a stretching cylinder, Int. J. Non-linear Sci. Numer. Simul. 16 (2015) 161–164.
[12] R. Ali, A. Shahzad, M. Khan, M. Ayub, Analytic and numerical solutions for axisymmetric flow with partial slip, Eng. Comput. 32 (2016) 149–154.
[13] B. Mahanthesh, B.J. Gireesha, R.S. Reddy Gorla, F.M. Abbasi, S.A. Shehzad, Numerical solutions for magnetohydrodynamic flow of nanofluid over a bidirectional non-linear stretching surface with prescribed surface heat flux boundary, J. Magnetism Magnetic Mater. 417 (2016) 189–196.
[14] T. Salahuddin, M.Y. Malik, Arif Hussain, S. Bilal, M. Awais, MHD flow of Cattanneo-Christov heat flux model for Williamson fluid over a stretching sheet with variable thickness: using numerical approach, J. Magnetism Magnetic Mater. 401 (2016) 991–997.
[15] M.Y. Malik, T. Salahuddin, Arif Hussain, S. Bilal, MHD flow of tangent hyperbolic fluid over a stretching cylinder: using Keller box method, J. Magnetism Magnetic Mater. 395 (2015) 271–276.
[16] M.Y. Malik, T. Salahuddin, Numerical solution of MHD stagnation point flow of Williamson fluid model over a stretching cylinder, Int. J. Nonlinear Sci. Numer. Simul. 16 (2015) 161–164.
[17] M.Y. Malik, Arif Hussain, T. Salahuddin, M. Awais, Numerical Solution of MHD Sisko fluid over a stretching cylinder and heat transfer analysis, Int. J. Numer. Methods Heat Fluid Flow, doi: http://dx.doi.org/10.1108/HFF-06-2015-0211.
[18] M.Y. Malik, A. Hussain, T. Salahuddin, M. Awais, S. Bilal, Magnetohydrodynamic flow of Sisko fluid over a stretching cylinder with variable thermal conductivity: a numerical study, AIP Adv. 6 (2016) 025316.
[19] M.Y. Malik, I. Khan, A. Hussain, T. Salahuddin, Mixed convection flow of MHD Eyring-Powell nanofluid over a stretching sheet; a numerical study, AIP Adv. 5 (2015) 117118.
[20] M.Y. Malik, A. Hussain, T. Salahuddin, M. Awais, Effects of viscous dissipation on MHD boundary layer flow of Sisko fluid over a stretching cylinder, AIP Adv. 6 (2016) 035009.
[21] T. Salahuddin, M.Y. Malik, A. Hussain, S. Bilal, M. Awais, Combined effects of variable thermal conductivity and MHD flow on pseudoplastic fluid over a stretching cylinder by using Keller box method, Inform. Sci. Lett. Int. J. 5 (2016) 11–19.
[22] T. Salahuddin, M.Y. Malik, A. Hussain, S. Bilal, M. Awais, Effects of transverse magnetic field with variable thermal conductivity on tangent hyperbolic fluid with exponentially varying viscosity, AIP Adv. 5 (2015) 127103.
[23] M.Y. Malik, M. Khan, T. Salahuddin, I. Khan, Variable viscosity and MHD flow in Casson fluid with Cattaneo–Christov heat flux model: using Keller box method, Eng. Sci. Technol., Int. J., doi: http://dx.doi.org/10.1016/j.jestch.2016.
[24] A.R.A. Khaled, K. Vafai, Hydromagnetic squeezed flow and heat transfer over a sensor surface, Int. J. Eng. Sci. 42 (2004) 509–519.
[25] M. Rashidi, H. Shahmohamadi, S. Dinarvand, M.M. Rashidi, H. Shahmohamadi, S. Dinarvand, Analytic approximate solutions for unsteady two-dimensional and axisymmetric squeezing flows between parallel plates, Math. Problems Eng. (2008) 935095.
[26] R.U. Haq, S. Nadeem, Z.H. Khan, N.F.M. Noor, MHD squeezed flow of water functionalized metallic nanoparticles over a sensor surface, Physica E 73 (2015) 45–53.
[27] M.Y. Malik, T. Salahuddin, A. Hussain, S. Bilal, M. Awais, Homogeneous-heterogeneous reactions in Williamson fluid

model over a stretching cylinder by using Keller box method, AIP Adv. 5 (10) (2015) 107227.
[28] M.Y. Malik, A. Hussain, T. Salahuddin, M. Awais, S. Bilal, F. Khan, Flow of Sisko fluid over a stretching cylinder and heat transfer with viscous dissipation and variable thermal conductivity: a numerical study, AIP Adv. 6 (4) (2016) 045118.
[29] M.Y. Malik, M. Bibi, F. Khan, T. Salahuddin, Numerical solution of Williamson fluid flow past a stretching cylinder and heat transfer with variable thermal conductivity and heat generation/absorption, AIP Adv. 6 (3) (2016) 035101.
[30] Khalil Ur Rehman, M.Y. Malik, T. Salahuddin, M. Naseer, Dual stratified mixed convection flow of Eyring-Powell fluid over an inclined stretching cylinder with heat generation/absorption effect, AIP Adv. 6 (2016) 075112.
[31] M.Y. Malik, A. Hussain, T. Salahuddin, M. Awais, S. Bilal, Numerical solution of Sisko fluid over a stretching cylinder and heat transfer with variable thermal conductivity, J. Mech., doi: http://dx.doi.org/10.1017/jmech.2016.8.
[32] T. Hayat, F.M. Abbasi, B. Ahmad, A. Alsaedi, Peristaltic transport of Carreau-Yasuda fluid in a curved channel with slip effects, Plos ONE, doi: http://dx.doi.org/10.1371/journal.pone.0095070.
[33] T. Hayat, F.M. Abbasi, A. Alsaedi, F. Alsaadi, Hall and Ohmic heating effects on the peristaltic transport of a Carreau–Yasuda fluid in an asymmetric channel, Zeitschrift Naturforschung A 69 (2014) 43–51.
[34] T. Hayat, A. Tanveer, A. Alsaedi, Mixed convective peristaltic flow of Carreau–Yasuda fluid with thermal deposition and chemical reaction, Int. J. Heat Mass Transfer 96 (2016) 474–481.

Please cite this article in press as: T. Salahuddin et al., MHD squeezed flow of Carreau-Yasuda fluid over a sensor surface, Alexandria Eng. J. (2016), http://dx.doi.org/10.1016/j.aej.2016.08.029